Published in final edited form as:
J Comp Neurol. 2009 November 10; 517(2): 134–145. doi:10.1002/cne.22148.

Distribution of High-Conductance Calcium-Activated Potassium Channels in Rat Vestibular Epithelia

Felix E. Schweizer[1,*], **David Savin**[1], **Cindy Luu**[1], **David R. Sultemeier**[2], and **Larry F. Hoffman**[2]

[1]Department of Neurobiology, David Geffen School of Medicine at UCLA, Los Angeles, California 90095

[2]Division of Head and Neck Surgery, David Geffen School of Medicine at UCLA, Los Angeles, California 90095

Abstract

Voltage- and calcium-activated potassium channels (BK) are important regulators of neuronal excitability. BK channels seem to be crucial for frequency tuning in nonmammalian vestibular and auditory hair cells. However, there are a paucity of data concerning BK expression in mammalian vestibular hair cells. We therefore investigated the localization of BK channels in mammalian vestibular hair cells, specifically in rat vestibular neuroepithelia. We find that only a subset of hair cells in the utricle and the crista ampullaris express BK channels. BK-positive hair cells are located mainly in the medial striolar region of the utricle, where they constitute at most 12% of hair cells, and in the central zone of the horizontal crista. A majority of BK-positive hair cells are encapsulated by a calretinin-positive calyx defining them as type I cells. The remainder are either type I cells encapsulated by a calretinin-negative calyx or type II hair cells. Surprisingly, the number of BK-positive hair cells in the utricle peaks in juvenile rats and declines in early adulthood. BK channels were not found in vestibular afferent dendrites or somata. Our data indicate that BK channel expression in the mammalian vestibular system differs from the expression pattern in the mammalian auditory and the nonmammalian vestibular system. The molecular diversity of vestibular hair cells indicates a functional diversity that has not yet been fully characterized. The predominance of BK-positive hair cells within the medial striola of juvenile animals suggests that they contribute to a scheme of highly lateralized coding of linear head movements during late development.

Indexing terms

utricle; crista ampullaris; hair cells; striola; calretinin; immunohistochemistry

Large-conductance, voltage- and calcium-activated potassium channels (BK channels, also known as $K_{Ca}1.1$, KCNMA1, Slo1 or maxi-K) are important contributors to neuronal excitability by, for example, regulating the duration of calcium action potential trains, shaping the after-hyperpolarization, and curtailing calcium entry at the presynaptic nerve terminal (Salkoff et al., 2006). They are frequently clustered together with calcium channels (Issa and Hudspeth, 1994; Samaranayake et al., 2004), especially at presynaptic terminals, where they might regulate synaptic transmission (Augustine et al., 1988; Roberts et al.,

[*]Correspondence to: Felix E. Schweizer, Department of Neurobiology, David Geffen School of Medicine at UCLA, 650 Charles E. Young Drive S., CHS 63-323, Los Angeles, CA 90095-1763. felixs@ucla.edu.

Additional Supporting Information may be found in the online version of this article.

1990; Robitaille et al., 1993). BK channels contribute to electrical tuning in auditory hair cells of amphibians, reptiles, and birds (Fettiplace and Fuchs, 1999), and variations in expression of BK α-subunit splice variants and β-subunits along the auditory epithelium parallel its tonotopic organization (Ramanathan et al., 1999). Vestibular hair cells of the frog sacculus, which also exhibit electrical tuning and have auditory characteristics in signaling ground vibrations (Smotherman and Narins, 2000), express BK channels that are clustered together with calcium channels at the release sites (Roberts et al., 1990). This arrangement suggests tuning not only of the electrical resonance but also of neurotransmitter release, a hypothesis that has recently received experimental support (Rutherford and Roberts, 2006).

Results from studies of BK function in mammalian hair cells do not yield a clear picture of their contribution to stimulus coding. Inner hair cells of the mammalian cochlea, which are not electrically tuned, do express BK channels that appear not to be activated by entry of extracellular calcium (Kros and Crawford, 1990) but rather by calcium released from intracellular stores (Marcotti et al., 2004) or even in a calcium-independent manner (Thurm et al., 2005). BK channels of rodent cochlear inner hair cells are not localized to the basal release sites, but rather toward their apical neck (Pyott et al., 2004, 2007; Hafidi et al., 2005). Furthermore, BK null mutant animals exhibit normal auditory brainstem responses and do not show an obvious vestibular phenotype (Pyott et al., 2007). The functional contribution of BK channels to mammalian inner ear function thus remains unclear.

In view of the morphologic and functional differences between inner ear hair cells of mammals and other vertebrates, the present study was undertaken to investigate the expression of BK channels in the mammalian vestibular system, focusing on the rat utricle. By using immunohistochemical methods, we found that only a small subset of vestibular hair cells express the pore-forming α-subunit of BK channels at detectable levels. No BK channel expression was found in the afferent dendrites or Scarpa's ganglion somata. The BK-positive hair cells were predominantly found in the utricular medial striola and in the semicircular canal crista central zone. More than half of the BK-positive hair cells were positively identified as type I, because they were surrounded by a calretinin-positive afferent calyx. BK channels were not clustered at the basal end (as in frog saccular hair cells), and although there was a prominence of labeling toward the apical side, it was—unlike in mammalian cochlear inner hair cells—not restricted to the apical portion. In addition, we found that BK channels start being expressed around eye-opening (Curthoys, 1979). Expression peaked around 3–4 weeks of age and then decayed to very low levels by 3 months. Our results suggest a surprising molecular heterogeneity of mammalian vestibular hair cells and argue for a functional specialization of the medial striola in lateralized signaling through a critical period of vestibular neuroepithelia development.

MATERIALS AND METHODS

Tissue preparation

Sprague-Dawley rats (age range: 6–102 days) were euthanized with isofluorane and decapitated following protocols approved by the UCLA Institutional Animal Care and Use Committee. The medial aspect of the temporal bone was rapidly exposed, and a fenestra was made in the caudal vestibule, through which fixative (4% paraformaldehyde in phosphate-buffered saline [PBS] pH 7.4) was gently infused. The bone was then dissected, and the fenestra widened for disruption of the membranous labyrinth, immersed in fixative, and incubated for 2 hours on an agitator. PBS was then infused into the fenestra, and the temporal bone was stored at 4°C until further dissection. For dissection, the utricle was exposed *in situ*; in paraformaldehyde-fixed specimens the otolithic membranes were easily removed by gently blowing streams of PBS over the utricular surfaces. After further resection of the bone, the utricle and horizontal crista were isolated, removed, and then

washed with PBS. (The cupula of the crista was removed with the trimming of the membranous labyrinth.) About 36 animals were used for the various labeling experiments. Each experiment was performed at least three times with tissue from at least three different animals.

Antibodies and stains

The following reagents were used throughout the study at the dilutions indicated unless otherwise stated in the text. The primary antibodies used were: mouse anti-BK, clone L6/60 (1:50; NeuroMab, Davis, CA) and rabbit anti-calretinin (1:500; Chemicon, Temecula, CA). The secondary antibodies and stains (all from Invitrogen, Carlsbad, CA) were: Alexa Fluor 568 goat anti-mouse-IgG2a (1:500), Alexa Fluor 488 goat anti-rabbit (1:500), NeuroTrace 500/525 green-fluorescent Nissl stain (1:250), NeuroTrace 640/660 deep red-fluorescent Nissl stain (1:250), and phalloidin-conjugated Alexa Fluor 488 (1:100).

Antibody specificity

The anti-BK monoclonal IgG2a antibody L6/60 used in this study was raised against a fusion protein of GST with amino acids 690–1,196 of the mouse Kcnma1 protein with the antibody binding mapping to amino acids 690–891 as determined by enzyme-linked immunosorbent assay (ELISA) and immunoblots (Misonou et al., 2006). This antibody has been shown not to cross-react with other bands on Western blots of a rat brain membrane fraction and does not recognize an antigen in BK-null mutant mice (Misonou et al., 2006). The antibody binding site falls within an invariant exon that is shared between the known rodent BK isoforms, and antigenicity does not appear to be affected by BK phosphorylation (Misonou et al., 2006). We further confirmed the specificity of the antibody in cerebellar and cochlear sections. Consistent with previous reports (Misonou et al., 2006; Sausbier et al., 2006), we found robust BK immunoreactivity in sections of rat cerebellum associated with the molecular layer and Purkinje cells but not in the granule cell layer (data not shown). In the rodent cochlea, again in accordance with previous work (Pyott et al., 2004), we observed punctuate staining in inner hair cells (data not shown). We did not detect any labeling of outer hair cells in the sections of cochlea that we obtained (data not shown).

The rabbit anti-calretinin antibody used in the present investigation (AB5054; Chemicon/Millipore) was raised against recombinant rat calretinin. We confirmed that this polyclonal antibody can clearly distinguish between calretinin and calbindin, a protein of very similar structure, by staining cryosections (see below for method) of rat cerebellum. Consistent with a large body of literature (for review, see Bastianelli, 2003), we observed robust labeling of granule cells with the anti-calretinin antibody, but detected no labeling in Purkinje cells that express calbindin (data not shown). Furthermore, the staining pattern that we observe in the rat utricle is consistent with the pattern observed by many laboratories in utricles of diverse species using several different sources of anti-calretinin antibodies (Desmadryl and Dechesne, 1992; Desai et al., 2005a; Li et al., 2008).

The antibody against β3-tubulin mentioned in the *Results* section was a polyclonal, affinity-purified antibody (Covance, Princeton, NJ, PRB-435P) raised in rabbits against the well-characterized TUJ1 epitope located at the C-terminal end of β3-tubulin (Lee et al., 1990). The six C-terminal amino acids of β3-tubulin conserved among rat, mouse, and human (EAQGPK) were linked via an additional cystein to the carrier keyhole limpet hemocyanin (KLH). This antibody recognizes a doublet of bands in spiral ganglion extracts (Flores-Otero et al., 2007) consistent with a post-translational modification of β3-tubulin detected by this antibody (Cicchillitti et al., 2008). In control experiments, we observed no staining of non-neuronal cells (i.e., support cells, hair cells, or transitional epithelium) in the utricular epithelium in the utricular epithelium when using this at a 1:250 dilution.

Secondary-only controls were routinely done alongside with regular staining to ascertain background fluorescence.

Whole-mount immunohistochemistry

In most cases, specimens were processed intact. Tissue was blocked with 10% normal goat serum (NGS; Invitrogen, Carlsbad, CA) and 2% Triton X-100 (TX-100) in PBS for 2 hours at room temperature. Specimens were then incubated in primary antibody in 1% NGS and 0.2% TX-100 in PBS for 36 hours, rinsed three times for 10 minutes in PBS, and incubated in secondary antibody in NGS/TX-100/PBS for 2 hours at room temperature. Specimens were then rinsed three times for 10 minutes in PBS, mounted with Vectashield Hardset mounting media containing DAPI (Vector, Burlingame, CA) on Superfrost Plus glass slides, coverslipped, and sealed with nail polish.

Cryosection immunohistochemistry

Following dissection, the tissue was cryoprotected overnight in 30% sucrose in PBS, placed in cryosectioning media (Tissue-Tek O.C.T. EMS, Hatfield, PA), and then frozen at −20°C. Serial sections (12 μm) were cut in a plane essentially orthogonal to the striola, yielding a significant number of sections that contained the striolar region in addition to medial and lateral extrastriola. Sections were mounted on glass microscope slides (SuperFrost/Plus, Thermo Scientific, Waltham, MA), which were then stored at −80°C.

Tissue sections were rehydrated in PBS for 1 hour at room temperature, and then blocked with 5% NGS, 0.1% TX-100 in PBS for 1 hour at room temperature. Sections were then incubated in primary antibody in blocking solution overnight at 4°C, rinsed three times for 10 minutes at room temperature with PBS, incubated in secondary antibody in blocking solution for 2 hours at room temperature, rinsed three times for 10 minutes in PBS, mounted with Vectashield Hardset mounting solution containing DAPI, coverslipped, and then sealed with nail polish.

Imaging and image analysis

Specimens were imaged by using standard epifluorescence and confocal laser scanning microscopy. Confocal images were captured on a Zeiss LSM 510 Meta confocal microscope implemented on an upright Axioplan 2 microscope. Zeiss LSM 510 software was used to capture images. The 488 (at 15% intensity) and 543 (at 80% intensity) laser lines were used for excitation. A bandpass filter of 505–530 nm was used for the green channel and a bandpass filter of 560–615 nm was used for the red channel. A Zeiss Plan-Neofluar 10×/0.3 NA objective was used to capture low-magnification images, and high-magnification images were obtained by using a Zeiss Plan-Apochromat 63×/1.4 NA oil-immersion objective with 1.5× scan zoom. Each image was scanned at 512 × 512 pixels. Confocal stacks were analyzed with Neurolucida (MBF Bioscience, Williston, VT), ImageJ (rsb.info.nih.gov/ij/), and/or Volocity (PerkinElmer/Improvision, Waltham, MA). The final figures were composed in Adobe Photoshop CS4 (Adobe Systems, San Jose CA). No adjustments were made in gain, contrast, or any other parameters for any of the quantitative assessments in staining. Linear gain/contrast settings were adjusted in Photoshop and Volocity only for Figure 4A and B, respectively.

RESULTS

We used a monospecific monoclonal antibody (L6/60, NeuroMab) against the α-subunit of the large-conductance, calcium- and voltage-dependent potassium channel (BK; $K_{Ca}1.1$, Slo1, KCNMA1; see Materials and Methods for specificity of the antibody) to localize BK channels in the vestibular neuroepithelia of rats. We first examined the distribution of BK

staining across the sensory epithelium of the utricle in juvenile animals (19–23 days old). In light of the BK staining of all cochlear inner hair cells, we expected most if not all utricular hair cells to express BK. Surprisingly however, we did not observe any staining above background levels in most parts of the utricular epithelium. Instead, the staining was limited to a fraction of hair cells located in an area of the epithelium (Fig. 1) reminiscent of the striolar region. The striola represents a crescent-shaped region of the utricular epithelium exhibiting morphological and physiological specializations (Desai et al., 2005b;Eatock and Lysakowski, 2006) and includes the “line” where the orientations of stereocilia bundles reverse (Flock, 1964;Li et al., 2008).

To investigate the topographic relationship between BK-positive hair cells and the striolar region, we determined their morphological polarization vectors (MPVs). For this, rat utricles were double-stained with BK antibodies and with the actin-filament marker phalloidin (Figs. 1, 2). Phalloidin predominantly stains the actin cytoskeleton associated with tight junctions and adherens junctions between hair cells and support cells (Nunes et al., 2006), revealing a web-like staining pattern. In addition, phalloidin also stains the actin-containing stereocilia in hair cells and the cuticular plate (DeRosier and Tilney, 1989), but not the kinocilium, which, being a true cilium, contains tubulin. Thus, there is an identifiable void where the kinocilium is located in the phalloidin-stained epithelium viewed at high magnification, (Fig. 2A, inset; Lu and Popper, 1998;Li et al., 2008). Multiple image stacks were taken at high resolution (63×, 1.5× digital zoom) throughout the striolar region. The MPV of each hair cell was then determined by locating the central point of its apical surface and drawing a vector to the kinocilium by using Neurolucida (MBF Bioscience, Williston, VT; Fig. 2A). A subsequent low-magnification scan (10×; Fig. 2B) indicated the location in the utricle where each image stack was taken due to the marked photo-bleaching. Hair cells with centrifugal MPVs, i.e., MPVs that are pointing away from the center of the head, were classified as medial (Fig. 2D, white arrows). Those with centripetal MPVs, i.e., MPVs that are pointing toward the center of the head, were classified as lateral (Fig. 2D, cyan arrows). The reversal line as indicated by the hair cell MPVs was determined (Fig. 2D,E, yellow line). Figure 2E shows an image plane deeper in the stack where the BK staining of hair cells could be assessed. Thus it was possible to determine whether a given BK-positive hair cell had a centrifugally or centripetally oriented MPV.

Figure 3 shows a composite of a utricular epithelium stained with phalloidin and anti-BK antibodies. On this low-power micrograph, all BK-positive hair cells with centrifugal MPVs are colored in white, whereas those with centripetally oriented MPVs are in red (Fig. 3). We found that a large majority of BK-positive hair cells (94 ± 2%; n = 3 utricles from three animals) were located in the medial striola, with centrifugally oriented MPVs (Fig. 3, inset; for each utricle the number of BK-positive hair cells located in the medial striola relative to all BK-positive hair cells in the striola was: 101 of 105, 74 of 79, and 111 of 120). By using the presence of calretinin-positive calyces as markers for the striolar region (Leonard and Kevetter, 2002;Desai et al., 2005b;Li et al., 2008), we counted a total number of about 800 hair cells in the striola (n = 3 utricles from three animals; 724, 808, 828), leading us to estimate that about 12% of the striolar hair cells are BK positive. Taken together, these data indicate that in the juvenile rat utricle, BK-positive hair cells make up a small fraction of hair cells within the striolar region and are not symmetrically organized around the reversal line (see also Li et al., 2008).

We next sought to determine whether the BK-positive hair cells in the medial striolar region were engulfed by a postsynaptic calyx and could thus be classified as type I. Calretinin has been suggested to localize specifically to calyces of afferents exhibiting calyx-only dendritic morphologies (but not to dimorphic afferents) in the striolar region (Desmadryl and

Dechesne, 1992; Leonard and Kevetter, 2002; Desai et al., 2005b), and we therefore investigated the association between BK-positive hair cells and calretinin-positive calyces.

Figure 4A is a low-power view of a utricle whole-mount preparation double stained for calretinin (green) and BK (red). Note again the crescent-shaped staining pattern (Fig. 4A, white arrows) of the BK antibody. Calretinin is present in striolar calyces, as well as some hair cells (Desai et al., 2005b; Li et al., 2008), which can only be discerned easily at higher magnification. Figure 4B shows a confocal section through a utricle stained as in Figure 4A. Note the presence of multiple calretinin-positive calyces (long arrows) and calretinin-positive hair cells (arrowhead). We determined that 62 ± 4% of the BK-positive hair cells were surrounded by a calretinin-positive calyx (Fig. 4B, long arrow, left), but not all calretinin-positive calyces contained a BK-positive hair cell (Fig. 4B, long arrow, right). We could not determine whether the remaining hair cells (Fig. 4B, short arrow) were associated with a calretinin-negative calyx or with no calyx at all, which would identify them as type II hair cells.

To confirm the type I identity of at least a fraction of BK-positive hair cells, we immunolabeled 12-μm cryostat sections, cut perpendicular to the macular epithelium to include the striolar region, with anti-calretinin and anti-BK antibodies. Stained sections were then viewed with the confocal microscope; a maximum intensity projection of a confocal stack is shown in Figure 4C. Similar to the whole-mount preparation, calretinin-positive calyces were again very prominent and frequently associated with BK-positive hair cells. Within individual hair cells, the staining appeared to be fairly uniform and clearly not restricted to either apical or basal regions, although enhanced staining in the very apical portion of the hair cells was frequently observed (Figs. 4C, 5). A majority of BK-positive hair cells were amphora-shaped and surrounded by a calretinin-positive calyx, clearly identifying them as type I (Fig. 4). However, numerous BK-positive hair cells were not associated with a calretinin-positive calyx, making their classification (i.e., type I or II) difficult with the immunofluorescence methods utilized in the present study. Figure 5A shows a serially sectioned specimen in which a BK-positive hair cell clearly exhibits type I morphology, but is not surrounded by a calretinin-positive calyx. The 3D volume rendering of such BK-positive hair cells further supports the interpretation that they represent type I hair cells (Fig. 5B). A small fraction of BK-positive hair cells that were not associated with a calretinin-positive calyx appeared more cylindrical, and their cell bodies and nuclei were located closer to the surface of the epithelium, as revealed by double-staining utricular sections with BK antibodies and NeuroTrace, a fluorescent Nissl stain (Fig. 5C,D). This suggests that some BK-positive hair cells are likely type II. To summarize, the majority of BK-positive hair cells are type I, and, consistent with their striolar localization, many of these are associated with a calretinin-positive calyx. A minority of BK-positive hair cells might be type II. Taken together, these results indicate a remarkable molecular diversity of hair cells in the vestibular epithelium revealed by querying even just two molecular markers.

Obviously, calretinin-positive calyces are emanating from calretinin-positive afferent parent axons and can be clearly discerned in the tissue underlying the sensory epithelium (data not shown).

Interestingly, we failed to identify any BK-positive fibers in this area. To confirm the absence of BK-positive afferent fibers, we double-stained sections of Scarpa's ganglion for calretinin and BK (Fig. 6). In serial sections through the entire ganglion we observed less than 1% cell bodies that exhibited BK immunoreactivity above background of adjacent cells (15 of 3,121 cell bodies, n = 3 ganglia from three 3-week-old animals). We also did not detect BK-positive cells in ganglia from adult animals (not shown). The BK-positive structures that are visible in the ganglion (Fig. 6) do not stain for β3-tubulin and are thus

unlikely to be of neuronal origin (data not shown). The absence of BK staining in vestibular afferent cell bodies and fibers stands in contrast to earlier studies that have reported functional expression of calcium-activated potassium channels in neurons enzymatically and mechanically dissociated from Scarpa's ganglia from young and adult rats (Limón et al., 2005). We do not understand the difference in the results, but it seems possible that isolation and/or culture conditions of Scarpa's ganglion somata altered the expression patterns of BK subunits. Alternatively, the activity recorded by Limón et al. (2005) might not be due to expression of the KCNMA1 α-subunit that is recognized by L6/60 (but see Materials and Methods and Discussion for antibody specificity). Finally, we note that different strains of rats, although both albino, were used (Sprague-Dawley here, Wistar in Limón et al.), and small differences in the vestibular architecture between these strains have been described (Lindenlaub and Oelschläger, 1999).

To address whether the sparse labeling of utricular hair cells for BK channels was due to the young age of the animals, we stained whole mounts of utricles at various ages (Fig. 7). We found no BK-positive hair cells in specimens from 6-day-old animals, which also did not yet exhibit mature-looking calretinin-positive calyces (Fig. 7A). At 12–15 postnatal days, we occasionally observed BK-positive hair cells in the emerging striolar region (Fig. 7B), and this staining became most pronounced at days 19–23 (Figs. 1–5, 7C). Surprisingly, in mature 2–3-month-old animals of either sex, rather than observing an increase in the number of BK-positive hair cells, we observed a pronounced decrease in BK-positive hair cells (Fig. 7D). As illustrated in Figure 7, it was the number of BK-positive hair cells, rather than the staining intensity that changed over this developmental time period.

To determine whether the selective labeling of only a subset of hair cells was specific to the utricular epithelium, we performed immunohistochemistry on the crista ampullaris of the semicircular canal from juvenile rats (P19–P23). Similar to the labeling in the utricle, only a small proportion of hair cells in the cristae were labeled with the BK antibody, as shown by the micrographs of horizontal cristae in Figure 8A–D. Many of the BK-positive hair cells in the horizontal crista were type I, as they were associated with a calretinin-positive calyx (Fig. 8D), and, similar to the utricle, the expression of BK was also restricted to an early developmental age. We did not detect any BK-positive hair cells in cristae from adult animals (Fig. 8E). BK-positive hair cells were located in the apex of the crista and were not found toward the lateral edges of the epithelium. The crista apex and utricular striola share certain morphologic (e.g., termination region of calyx-only, calretinin-positive afferents; Fernandez et al., 1988; Dechesne et al., 1994; Desai et al., 2005b) and physiologic (e.g., source of phasic afferents; Baird et al., 1988; Goldberg et al., 1990a,b) characteristics. The addition of BK-positive hair cells to this list underscores a role, if even a transient one, in support of phasic response dynamics.

DISCUSSION

In this study we investigated the presence and localization of the calcium- and voltage-activated potassium channel, BK, in the rat peripheral vestibular system. We focused our analysis on BK expression in the sensory epithelium of the utricle and of the crista of the horizontal semicircular canal. We found that BK expression in the rat utricle as reported by the L6/60 monoclonal antibody is restricted to a subset of mainly type I hair cells receiving the projection of a calretinin-positive calyx. The remainder of BK-positive hair cells are comprised of type I cells associated with calretinin-negative calyces and type II hair cells. We frequently observed a calretinin-positive afferent fiber ensheathing two adjacent hair cells, only one of which was BK positive (Figs. 4, 7C). This underscores the notion that most afferent fibers, not just dimorphic fibers, can integrate information from hair cells with distinct molecular, and perhaps physiological, characteristics. Synaptic integration at the

level of the first sensory synapse could thus convey to afferent fibers signaling properties that do not have a direct counterpart in any particular hair cell.

The L6/60 monoclonal antibody used in this study has been well characterized in terms of specificity in recognizing the pore-forming α-subunit of BK channels and does not cross-react with other proteins on either Western blots or tissue sections of BK-null mutant animals (Pyott et al., 2004; Misonou et al., 2006). The antibody binding epitope maps to an exon that is incorporated into all the known isoforms of the channel (Misonou et al., 2006), making it unlikely that specific splicing variants would elude detection. However, it is impossible to demonstrate that the antibody recognizes the BK protein under all circumstances. Thus the restricted BK immunoreactivity we observe could theoretically be due to an obstruction of the antibody binding site by an interacting protein and/or by post-translational modification(s). However, even in this case the BK-positive hair cells would identify a subset of vestibular hair cells that are molecularly distinct from other hair cells. An occlusion of immunoreactivity by interacting proteins or post-translational modifications would be interesting in its own right. It might also explain why we failed to detect immunoreactivity in afferents (i.e., either in the stromal fibers or Scarpa's ganglion somata) whereas Limón et al. (2005) detected functional calcium-activated potassium currents in cultured ganglion cells. Obviously, culturing can also change expression patterns of proteins, and a resolution of this discrepancy must await further study.

We report that in sensory epithelia of the utricle and the semicircular canals, expression of BK channels is restricted to a central part of the epithelium—the medial striola in the utricle and the central zone in the crista. These areas have been recognized as being morphologically and physiologically distinct from the surrounding sensory epithelium and are also innervated by distinct afferents (Lindeman, 1969; Baird et al., 1988; Fernandez et al., 1988, 1990; Lysakowski and Goldberg, 1997; Li et al., 2008; see also Ramón y Cajal, 1995; Goldberg, 2000). Afferent vestibular nerve fibers can be classified by their spontaneous discharge regularity (reviewed in Goldberg, 2000). Irregularly discharging afferents tend to innervate the central zone or striola and have a high sensitivity to stimulation. Furthermore, they have strong phasic response dynamics compared with the more tonic response of the regularly discharging fibers. Whereas the electrical properties of afferent nerve fibers contribute to their firing properties (Eatock et al., 2008), synaptic transmission will, through both pre- and postsynaptic components, strongly shape afferent firing characteristics. BK channels are usually co-localized with calcium channels and can serve as a negative feedback loop to truncate depolarization-induced calcium influx and thus limit exocytosis (Roberts et al., 1990; Robitaille et al., 1993; Issa and Hudspeth, 1994). Hair cells that express BK channels might thus be particularly tuned to encode phasic stimuli, a feature that is thought to be at least in part conveyed by afferents contacting hair cells located in the striola (Lysakowski and Goldberg, 2004). In any case, even just looking at two markers, BK channels and calretinin, yields in rats all possible combinations of labeling (e.g., Fig 2). This emerging picture of molecular diversity of vestibular hair cells might contribute substantially to defining the signal transfer between hair bundles and afferent fibers.

Vertebrate auditory epithelia and the frog saccule express functional BK channels in most if not all hair cells (Holt and Eatock, 1995; Smotherman and Narins, 1999; Hafidi et al., 2005) or at least all inner hair cells (Pyott et al., 2004). It is generally assumed that they are co-localized with calcium channels at neurotransmitter release sites. Calcium influx through the voltage-dependent calcium channels triggers neurotransmitter release and activates BK channels. The large outward potassium current through the BK channel then contributes to the repolarization of the terminal and terminates release. BK channels thus also contribute to electrical tuning in frog, avian, and turtle hair cells (Fettiplace and Fuchs, 1999) and their

alternative splicing appears to be regulated along the tonotopic axis (Navaratnam et al., 1997; Ramanathan et al., 1999). Interestingly, however, in the mammalian auditory system, BK channels are not localized at the basal end of hair cells where they could shape neurotransmitter release (Pyott et al., 2004; see Introduction). In the utricle and in the crista ampullaris of the horizontal canal, we find that BK channel expression is restricted to neither apical or basal portions, although on occasion we observed slightly stronger staining toward the hair cell apex. In addition, a large portion of the antigen appears to be located in an intracellular compartment. We do not know whether this represents channels that were never integrated due to a lack of appropriate β-subunits or whether they reflect a high turnover rate of surface-exposed BK channels.

Surprisingly, BK channel expression was not symmetrical around the hair bundle reversal line but was rather restricted to the medial side (Fig. 3). This signifies that the information conveyed by these molecularly distinct hair cells is not bilaterally symmetrical and raises the distinct possibility that signals reaching the central nervous system might also not be bilaterally symmetrical. This interpretation is supported by the finding of unequal concentrations of early developmental markers on either side of the reversal line (Deans et al., 2007) and by the recent report that calretinin-positive afferents project to hair cells medial of the reversal line (Li et al., 2008). Thus, although it has been generally assumed that the striola, characterized by hair cell and afferent fiber specializations (Flock, 1964;Lysakowski and Goldberg, 2004;Eatock and Lysakowski, 2006) is bisected by the reversal line, it now appears that this area is better defined by a location medial of the reversal line (Li et al., 2008).

Unexpectedly, we found that BK expression is maximal in juvenile animals and precipitously decreases in younger as well as older animals (Fig. 7). By 2 months of age we barely detected any immunoreactivity for BK in the utricle (Fig. 7D) and even that minimal staining was absent at 3 months (not shown). It is unlikely that barriers to antibody penetration were responsible for the absence of BK labeling in very young and older animals, as we did not observe any differences in the labeling efficacy at any age when BK-positive hair cells were observed, and because anti-calretinin antibodies gave robust staining into the depths of the specimens at all ages examined (Fig. 7). We offer the hypothesis that BK expression precedes eye-opening (Curthoys, 1979) and peaks during maturation of the vestibular periphery. It will be interesting to investigate how BK expression contributes to the refinement of vestibular function.

Although Curthoys (1982) has reported on the development of semicircular canal afferent discharge characteristics in rats, there is a glaring paucity of parallel information regarding utricular afferents. Furthermore, there is virtually no information regarding the development of vestibular reflexes in rats, although some insight can be gleaned from a more recent study of horizontal vestibulo-ocular reflex (VOR) in mice (Faulstich et al., 2004). Curthoys (1982) found that horizontal semicircular canal afferents gain achieved near-adult values by approximately P6, although response phases remained lower (i.e., larger phase lag re: peak stimulus) than afferents recorded from adults. The phase characteristic continued to mature in canal afferents through adulthood. If the developmental parallels can be drawn, our data suggest that BK expression in vestibular hair cells is uncorrelated to the development of adequate response magnitudes, although it may be associated with the maturation of the afferent response phase. In view of the general effect of BK on truncation of depolarization, this would have the effect of increasing the phase of the generator potential in afferent neurons, making it more adult-like in a fraction of afferents projecting onto BK-positive hair cells. The attenuation of BK expression in adult specimens clearly indicates that this contribution is assumed by other mechanisms in the transduction cascade.

Faulstich et al. (2004) have reported continued maturation of the angular VOR in mice between P21 and adulthood. It is not known whether this was driven by further maturity of the peripheral or central vestibular systems in these animals. This developmental stage in the mouse is likely to be comparable to rats of slightly older postnatal age. These data underscore, however, that the developmental period between P14 and P28 is a critical one in the development of labyrinthine circuits in rats and mice, in which the expression of BK in vestibular hair cells may play a crucial role.

If BK channels perform an important function in shaping the signaling properties of hair cells and thus afferent fibers, one would expect to unravel major auditory and vestibular deficits in BK-null mutant animals. However, despite intense investigation, no such deficits or changes were found in hair cells (Pyott et al., 2007), although afferent auditory fibers showed decreased maximal spike rates and decreased timing precision due to the loss of BK channels (Oliver et al., 2006). Similar studies remain to be conducted in the vestibular system, and their behavioral consequence remains to be fully tested.

Independent of the physiological role of BK channels in the vestibular system, we have used immunohistochemistry directed against BK to reveal a heretofore underappreciated heterogeneity of hair cells in the rat utricle and horizontal canal. Furthermore, BK-positive hair cells are located medial of the reversal line, indicating that information conveyed by these cells is not bilaterally symmetrical and thus challenging the current textbook notion of vestibular signaling.

Supplementary Material

Refer to Web version on PubMed Central for supplementary material.

Acknowledgments

The authors are grateful to Linda Nguyen for counting cells, Dr. Ivan Lopez for providing histologic sections of the rat cochlea, and Drs. Yuki Quinones and Nick Brecha for critical reading of the manuscript.

Grant sponsor: National Institute on Deafness and Other Communication Disorders, National Institutes of Health; Grant numbers: DC007678 (to F.E.S) and DC005801 (to L.F.H. and D.S); Grant sponsor: the Victor Goodhill Ear Research Foundation (to L.F.H. and D.S).

The monoclonal antibody L6/60 was obtained from the UC Davis/National Institute of Neurological Disorders and Stroke/National Institute of Mental Health NeuroMab Facility, which is supported by National Institutes of Health grant U24N2050606 and maintained by the Section of Neurobiology, Physiology and Behavior, College of Biological Sciences, University of California, Davis, CA 95616.

LITERATURE CITED

Augustine GJ, Charlton MP, Horn R. Role of calcium-activated potassium channels in transmitter release at the squid giant synapse. J Physiol (Lond). 1988; 398:149–164. [PubMed: 2455797]

Baird RA, Desmadryl G, Fernandez C, Goldberg JM. The vestibular nerve of the chinchilla. II. Relation between afferent response properties and peripheral innervation patterns in the semicircular canals. J Neurophysiol. 1988; 60:182–203. [PubMed: 3404216]

Bastianelli E. Distribution of calcium-binding proteins in the cerebellum. Cerebellum. 2003; 2:242–262. [PubMed: 14964684]

Cicchillitti L, Penci R, Di Michele M, Filippetti F, Rotilio D, Donati MB, Scambia G, Ferlini C. Proteomic characterization of cytoskeletal and mitochondrial class III $\in^2$-tubulin. Mol Cancer Ther. 2008; 7:2070–2079. [PubMed: 18645017]

Curthoys IS. The development of function of horizontal semicircular canal primary neurons in the rat. Brain Res. 1979; 167:41–52. [PubMed: 455071]

Curthoys IS. Postnatal developmental changes in the response of rat primary horizontal semicircular canal neurons to sinusoidal angular accelerations. Exp Brain Res. 1982; 47:295–300. [PubMed: 7117454]

Deans MR, Antic D, Suyama K, Scott MP, Axelrod JD, Goodrich LV. Asymmetric distribution of prickle-like 2 reveals an early underlying polarization of vestibular sensory epithelia in the inner ear. J Neurosci. 2007; 27:3139–3147. [PubMed: 17376975]

Dechesne CJ, Rabejac D, Desmadryl G. Development of calretinin immunoreactivity in the mouse inner ear. J Comp Neurol. 1994; 346:517–529. [PubMed: 7983242]

DeRosier DJ, Tilney LG. The structure of the cuticular plate, an in vivo actin gel. J Cell Biol. 1989; 109:2853–2867. [PubMed: 2592408]

Desai SS, Ali H, Lysakowski A. Comparative morphology of rodent vestibular periphery. II. Cristae ampullares. J Neurophysiol. 2005a; 93:267–280. [PubMed: 15240768]

Desai SS, Zeh C, Lysakowski A. Comparative morphology of rodent vestibular periphery. I. Saccular and utricular maculae. J Neurophysiol. 2005b; 93:251–266. [PubMed: 15240767]

Desmadryl G, Dechesne CJ. Calretinin immunoreactivity in chinchilla and guinea pig vestibular end organs characterizes the calyx unit subpopulation. Exp Brain Res. 1992; 89:105–108. [PubMed: 1601088]

Eatock, RA.; Lysakowski, A. Mammalian vestibular hair cells. In: Eatock, RA.; Fay, RR.; Popper, AN., editors. Vertebrate hair cells. New York: Springer; 2006. p. 348-442.

Eatock RA, Xue J, Kalluri R. Ion channels in mammalian vestibular afferents may set regularity of firing. J Exp Biol. 2008; 211:1764–1774. [PubMed: 18490392]

Faulstich BM, Onori KA, du Lac S. Comparison of plasticity and development of mouse optokinetic and vestibulo-ocular reflexes suggests differential gain control mechanisms. Vision Res. 2004; 44:3419–3427. [PubMed: 15536010]

Fernandez C, Baird RA, Goldberg JM. The vestibular nerve of the chinchilla. I. Peripheral innervation patterns in the horizontal and superior semicircular canals. J Neurophysiol. 1988; 60:167–181. [PubMed: 3404215]

Fernandez C, Goldberg JM, Baird RA. The vestibular nerve of the chinchilla. III. Peripheral innervation patterns in the utricular macula. J Neurophysiol. 1990; 63:767–780. [PubMed: 2341875]

Fettiplace R, Fuchs PA. Mechanisms of hair cell tuning. Annu Rev Physiol. 1999; 61:809–834. [PubMed: 10099711]

Flock Å. Structure of the macula utriculi with special reference to directional interplay of sensory responses as revealed by morphological polarization. J Cell Biol. 1964; 22:413–431. [PubMed: 14203389]

Flores-Otero J, Xue HZ, Davis RL. Reciprocal regulation of presynaptic and postsynaptic proteins in bipolar spiral ganglion neurons by neurotrophins. J Neurosci. 2007; 27:14023–14034. [PubMed: 18094241]

Goldberg JM. Afferent diversity and the organization of central vestibular pathways. Exp Brain Res. 2000; 130:277–297. [PubMed: 10706428]

Goldberg JM, Desmadryl G, Baird RA, Fernandez C. The vestibular nerve of the chinchilla. IV. Discharge properties of utricular afferents. J Neurophysiol. 1990a; 63:781–790. [PubMed: 2341876]

Goldberg JM, Desmadryl G, Baird RA, Fernandez C. The vestibular nerve of the chinchilla. V. Relation between afferent discharge properties and peripheral innervation patterns in the utricular macula. J Neurophysiol. 1990b; 63:791–804. [PubMed: 2341877]

Hafidi A, Beurg M, Dulon D. Localization and developmental expression of BK channels in mammalian cochlear hair cells. Neuroscience. 2005; 130:475–484. [PubMed: 15664704]

Holt JR, Eatock RA. Inwardly rectifying currents of saccular hair cells from the leopard frog. J Neurophysiol. 1995; 73:1484–1502. [PubMed: 7543944]

Issa NP, Hudspeth AJ. Clustering of Ca2+ channels and Ca(2+)-activated K+ channels at fluorescently labeled presynaptic active zones of hair cells. Proc Natl Acad Sci U S A. 1994; 91:7578–7582. [PubMed: 8052623]

Kros CJ, Crawford AC. Potassium currents in inner hair cells isolated from the guinea-pig cochlea. J Physiol. 1990; 421:263–291. [PubMed: 2348394]

Lee MK, Tuttle JB, Rebhun LI, Cleveland DW, Frankfurter A. The expression and posttranslational modification of a neuron-specific beta-tubulin isotype during chick embryogenesis. Cell Motil Cytoskel. 1990; 17:118–132.

Leonard RB, Kevetter GA. Molecular probes of the vestibular nerve: I. Peripheral termination patterns of calretinin, calbindin and peripherin containing fibers. Brain Res. 2002; 928:8–17. [PubMed: 11844467]

Li A, Xue J, Peterson EH. Architecture of the mouse utricle: macular organization and hair bundle heights. J Neurophysiol. 2008; 99:718–733. [PubMed: 18046005]

Limón A, Perez C, Vega R, Soto E. Ca2+-activated K+-current density is correlated with soma size in rat vestibular-afferent neurons in culture. J Neurophysiol. 2005; 94:3751–3761. [PubMed: 16107534]

Lindeman HH. Regional differences in structure of the vestibular sensory regions. J Laryngol Otol. 1969; 83:1–17. [PubMed: 4974740]

Lindenlaub T, Oelschläger HA. Morphological, morphometric, and functional differences in the vestibular organ of different breeds of the rat (*Rattus norvegicus*). Anat Rec. 1999; 255:15–19. [PubMed: 10321989]

Lu Z, Popper AN. Morphological polarizations of sensory hair cells in the three otolithic organs of a teleost fish: fluorescent imaging of ciliary bundles. Hear Res. 1998; 126:47–57. [PubMed: 9872133]

Lysakowski A, Goldberg JM. A regional ultrastructural analysis of the cellular and synaptic architecture in the chinchilla cristae ampullares. J Comp Neurol. 1997; 389:419–443. [PubMed: 9414004]

Lysakowski, A.; Goldberg, JM. Morphophysiology of the vestibular periphery. In: Highstein, SM.; Fay, RR.; Popper, AN., editors. The vestibular system. New York: Springer; 2004. p. 57-152.

Marcotti W, Johnson SL, Kros CJ. Effects of intracellular stores and extracellular Ca(2+) on Ca(2+)-activated K(+) currents in mature mouse inner hair cells. J Physiol. 2004; 557:613–633. [PubMed: 15064328]

Misonou H, Menegola M, Buchwalder L, Park EW, Meredith A, Rhodes KJ, Aldrich RW, Trimmer JS. Immunolocalization of the Ca2+-activated K+ channel Slo1 in axons and nerve terminals of mammalian brain and cultured neurons. J Comp Neurol. 2006; 496:289–302. [PubMed: 16566008]

Navaratnam DS, Bell TJ, Tu TD, Cohen EL, Oberholtzer JC. Differential distribution of Ca2+-activated K+ channel splice variants among hair cells along the tonotopic axis of the chick cochlea. Neuron. 1997; 19:1077–1085. [PubMed: 9390520]

Nunes FD, Lopez LN, Lin HW, Davies C, Azevedo RB, Gow A, Kachar B. Distinct subdomain organization and molecular composition of a tight junction with adherens junction features. J Cell Sci. 2006; 119:4819–4827. [PubMed: 17130295]

Oliver D, Taberner AM, Thurm H, Sausbier M, Arntz C, Ruth P, Fakler B, Liberman MC. The role of BKCa channels in electrical signal encoding in the mammalian auditory periphery. J Neurosci. 2006; 26:6181–6189. [PubMed: 16763026]

Pyott SJ, Glowatzki E, Trimmer JS, Aldrich RW. Extrasynaptic localization of inactivating calcium-activated potassium channels in mouse inner hair cells. J Neurosci. 2004; 24:9469–9474. [PubMed: 15509733]

Pyott SJ, Meredith AL, Fodor AA, Vazquez AE, Yamoah EN, Aldrich RW. Cochlear function in mice lacking the BK channel alpha, beta1, or beta4 subunits. J Biol Chem. 2007; 282:3312–3324. [PubMed: 17135251]

Ramanathan K, Michael TH, Jiang GJ, Hiel H, Fuchs PA. A molecular mechanism for electrical tuning of cochlear hair cells. Science. 1999; 283:215–217. [PubMed: 9880252]

Ramón, y; Cajal, S. Histology of the nervous system of man and vertebrates. In: Swanson, N.; Swanson, LW., translators. Original title: Histologie du systéme nerveaux de l'homme et des vertébrés. New York: Oxford University Press; 1995. p. 1909-1911.

Roberts WM, Jacobs RA, Hudspeth AJ. Colocalization of ion channels involved in frequency selectivity and synaptic transmission at presynaptic active zones of hair cells. J Neurosci. 1990; 10:3664–3684. [PubMed: 1700083]

Robitaille R, Garcia ML, Kaczorowski GJ, Charlton MP. Functional colocalization of calcium and calcium-gated potassium channels in control of transmitter release. Neuron. 1993; 11:645–655. [PubMed: 7691106]

Rutherford MA, Roberts WM. Frequency selectivity of synaptic exocytosis in frog saccular hair cells. Proc Natl Acad Sci U S A. 2006; 103:2898–2903. [PubMed: 16473940]

Salkoff L, Butler A, Ferreira G, Santi C, Wei A. High-conductance potassium channels of the SLO family. Nat Rev Neurosci. 2006; 7:921–931. [PubMed: 17115074]

Samaranayake H, Saunders JC, Greene MI, Navaratnam DS. Ca(2+) and K(+) (BK) channels in chick hair cells are clustered and colocalized with apical-basal and tonotopic gradients. J Physiol. 2004; 560:13–20. [PubMed: 15272029]

Sausbier U, Sausbier M, Sailer CA, Arntz C, Knaus HG, Neuhuber W, Ruth P. Ca2+ -activated K+ channels of the BK-type in the mouse brain. Histochem Cell Biol. 2006; 125:725–741. [PubMed: 16362320]

Smotherman MS, Narins PM. The electrical properties of auditory hair cells in the frog amphibian papilla. J Neurosci. 1999; 19:5275–5292. [PubMed: 10377339]

Smotherman MS, Narins PM. Hair cells, hearing and hopping: a field guide to hair cell physiology in the frog. J Exp Biol. 2000; 203(Pt 15):2237–2246. [PubMed: 10887064]

Thurm H, Fakler B, Oliver D. Ca2+-independent activation of BKCa channels at negative potentials in mammalian inner hair cells. J Physiol. 2005; 569:137–151. [PubMed: 16150795]

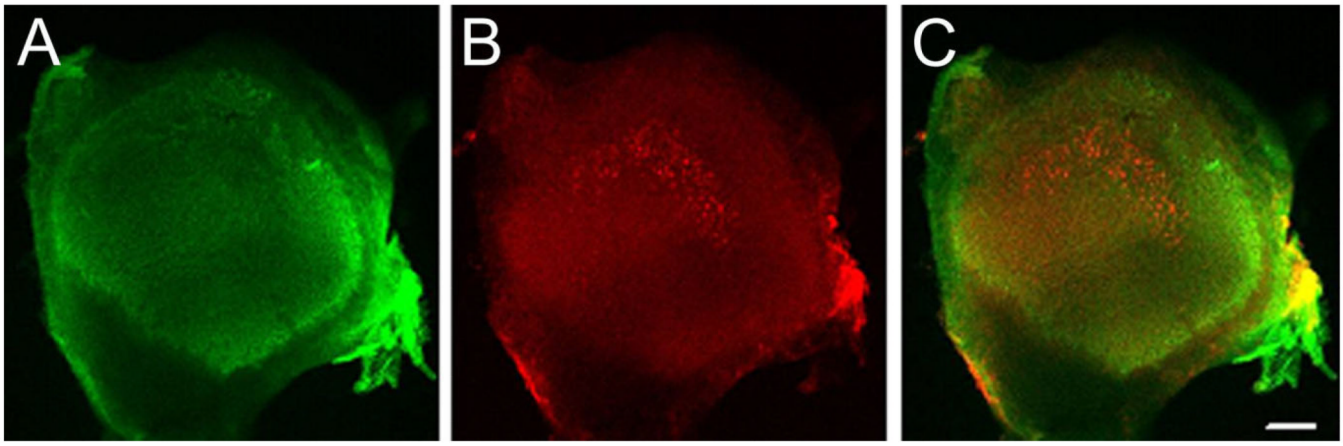

Figure 1.

Localization of BK immunoreactivity in rat utricle. Whole-mount preparation of rat utricle (postnatal day 21) double stained with (**A**) phalloidin (green, left) and (**B**) anti-BK antibodies (red, middle). **C:** Overlay of both images. Positive BK staining suggests striolar localization of BK. The images are maximum intensity projections of confocal image stacks obtained with a 10× objective. Magenta-green versions of all figures are available online. Scale bar = 100 μm in C (applies to A–C).

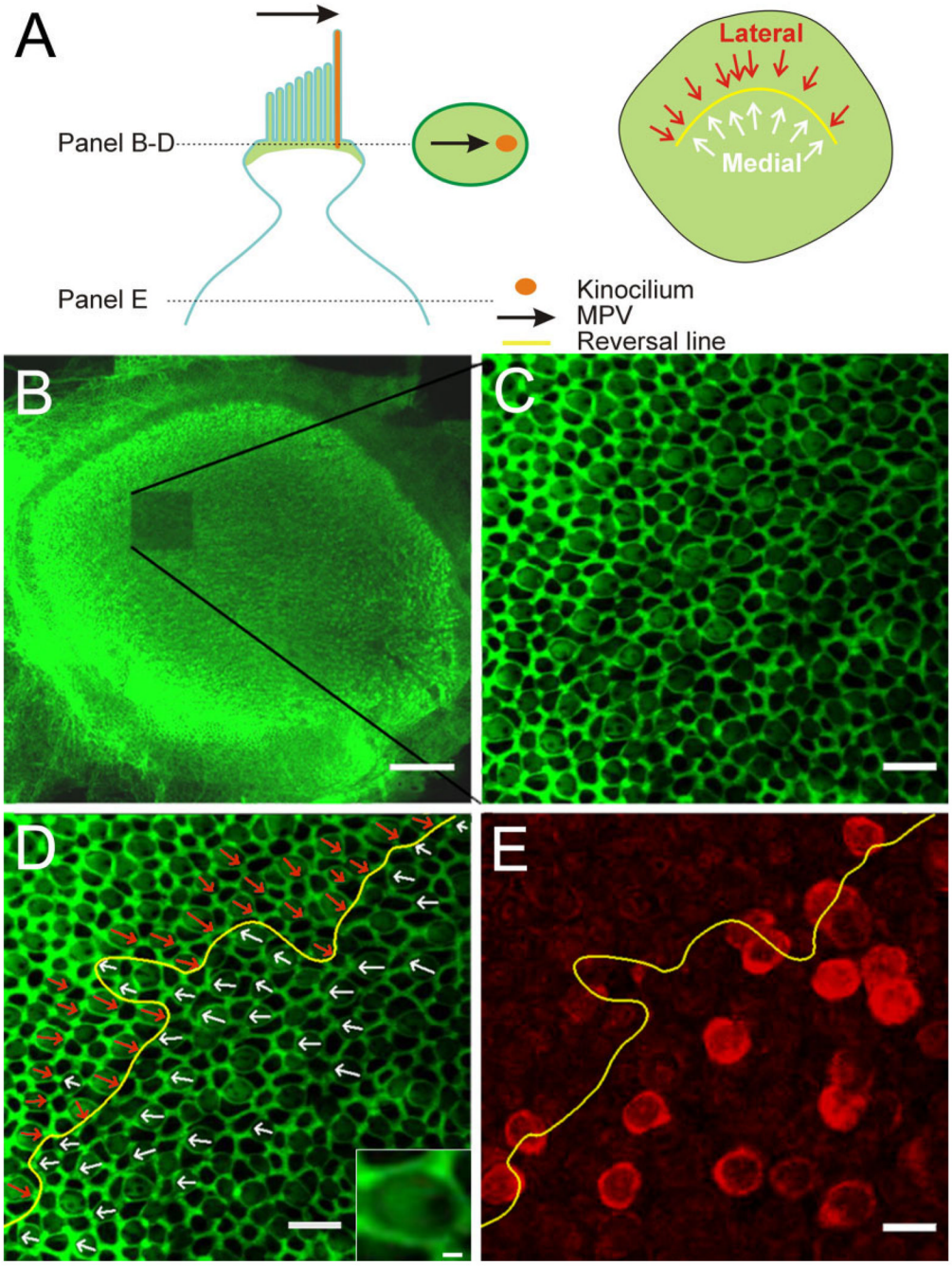

Figure 2.

Determination of the morphological polarization vector (MPV) and topographic localization of BK-positive hair cells. **A:** Schematic of an apical portion of a hair cell with the MPV (black arrow) pointing toward the kinocilium (orange). Stereocilia and the cuticular plate contain actin and lateral tight/adherens-junctions are associated with actin (green). The oval in the middle of illustrates a confocal section through the upper part of a hair cell. Actin staining creates a bright green surround (tight and adherens junctions), a lighter “fill” of the surround (base of stereocilia and cuticular plate), and a void (base of kinocilium). The MPV can thus be determined (black arrow). The schematic on the right shows the orientation of individual MPVs superimposed onto the utricular epithelium; the “reversal line” separates

the two orientations (yellow line). **B:** Low-magnification confocal image of a phalloidin-stained utricle after one stack of high-magnification images was acquired (note bleached region). **C:** Single confocal section at higher magnification. Note the honeycomb pattern of the tight and adherens junctions between cells and the fainter phalloidin staining in between, revealing a clear void, indicating the location of the kinocilium. **D:** Same image as in C but with the MPVs for centrifugal (white arrows) and centripetal (red arrows) hair cells superimposed. The reversal line is indicated in yellow. Inset shows a magnified view of a hair cell to illustrate the “actin void” on the right side. **E:** A confocal section from the same stack but deeper into the tissue. The BK staining (red) is now apparent and the reversal line determined in D is superimposed. Note that because hair cells are not necessarily oriented orthogonal to the imaging plane, the location of the cell body does not give a clear indication of the MPV orientation for that hair cell. Scale bar = 100 μm in B; 10 μm in C–E; 1 μm in inset in D.

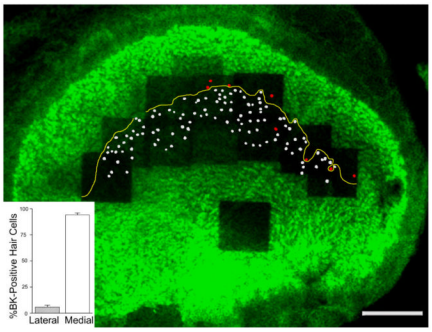

Figure 3.

Predominant localization of BK-positive hair cells on the medial side of the reversal line (yellow line). Hair cell tracings that have a lateral pointing MPV and thus are medial of the reversal line are indicated in white, whereas those that have a medial pointing MPV are colored in red. BK-positive hair cell quantification (inset) indicates that 94 ± 2% (n = 3 utricles from three animals) of all BK-positive hair cells in the utricle are medial of the reversal line. Note the single “orphan” hair cell with a medial-pointing MPV located medial to the reversal line. Scale bar = 100 μm).

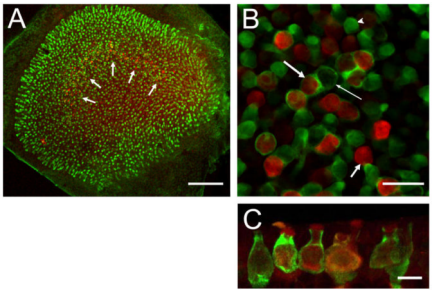

Figure 4.

Co-localization of BK channels (red) and calretinin (green). **A:** Whole-mount preparation viewed under low magnification. Many hair cells across the entire epithelium are calretinin positive (green), and a few calretinin-positive calyces can be discerned in the striolar region where a “band” of BK-positive hair cells is visible (white arrows). **B:** High-magnification view of striolar region. Note BK-positive hair cells surrounded (long, thick arrow) and not surrounded (short, thick arrow) by calretinin-positive calyces. Calretinin-positive calyces also surround BK-negative hair cells (thin arrow), and many calretinin-positive hair cells are visible (arrowhead). Of the BK-positive hair cells, 62 ± 4% (n = 3 utricles from 3 animals) are surrounded by a calretinin-positive calyx, characterizing them as type I. **C:** Maximum intensity projection of confocal images of cryostat section through the striolar region highlighting calyces and BK staining throughout hair cell (especially prominent at apical edge). Scale bar = 100 μm in A; 20 μm in B; 10 μm in C.

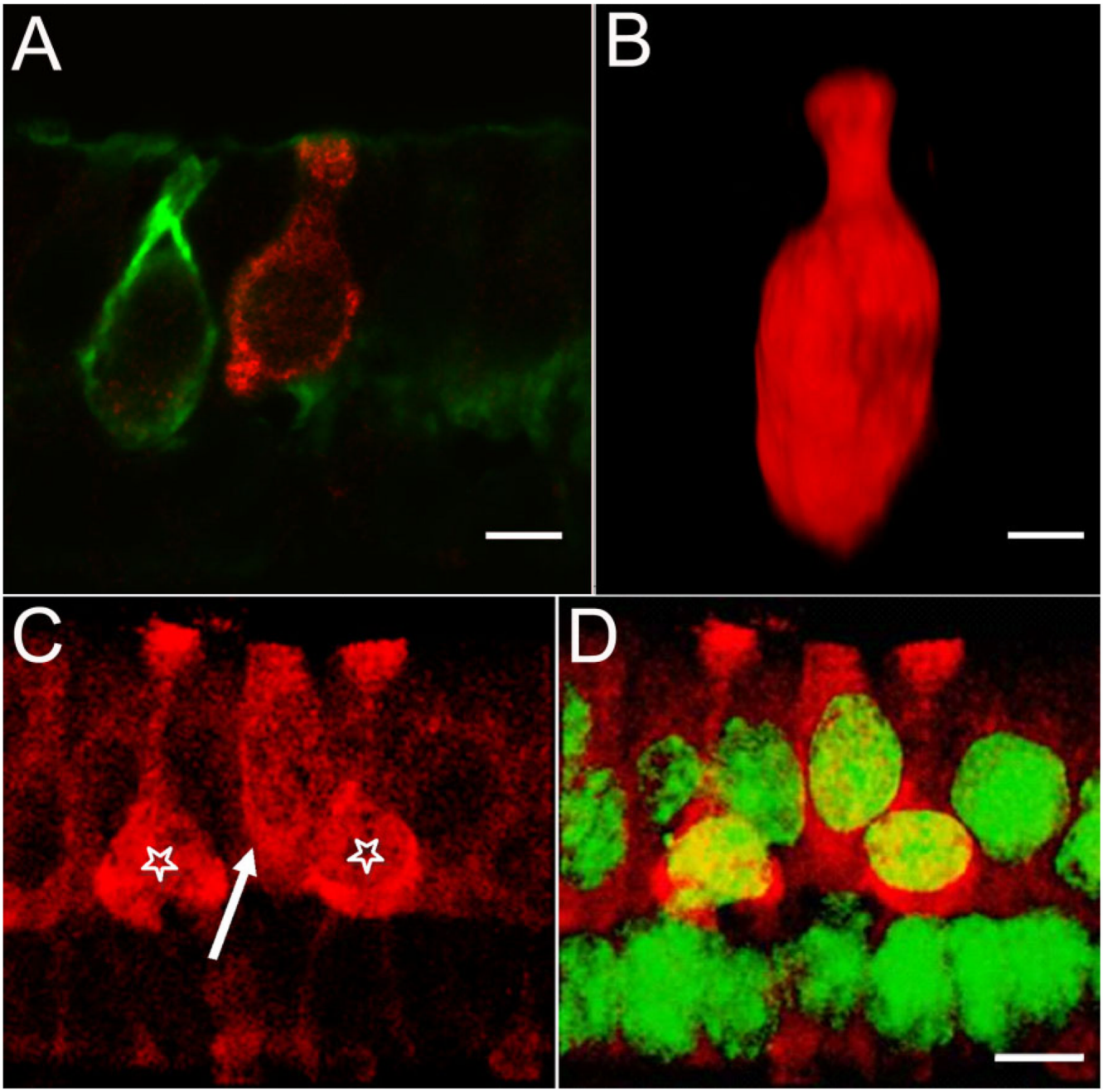

Figure 5.

Diversity of BK-positive hair cells. Serially sectioned specimens immunolabeled with anti-BK (red) and anti-calretinin (green) antibodies illustrate the diversity of BK-positive hair cells. **A:** An example of a BK-positive type I hair cell not encapsulated by a calretinin-positive calyx. The BK-positive hair cell exhibits the flask-shaped morphology indicative of a type I hair cell. Note the absence of BK-labeling in the adjacent hair cell enveloped by the calretinin-positive calyx. **B:** Three-dimensional volume reconstruction of a BK-positive hair cell from a different specimen. The classical type I morphology of this hair cell can be clearly appreciated. **C:** A putative BK-positive type II cell (arrow) next to two BK-positive type I cells (stars). **D:** Same image as in C, but with superimposed nuclear staining

(NeuroTrace, green). Note the apical localization of the nucleus for the putative type II hair cell. Scale bar = 5 μm.

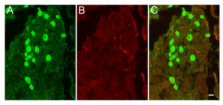

Figure 6.

Absence of BK immunoreactivity in Scarpa's ganglion. Cryosections through Scarpa's ganglion were double stained for (**A**) calretinin (green, left) and (**B**) BK (red, middle). **C:** Superposition of images shown in A and B. Note the absence of BK-positive cell bodies even at high exposure times. Scale bar = 10 μm.

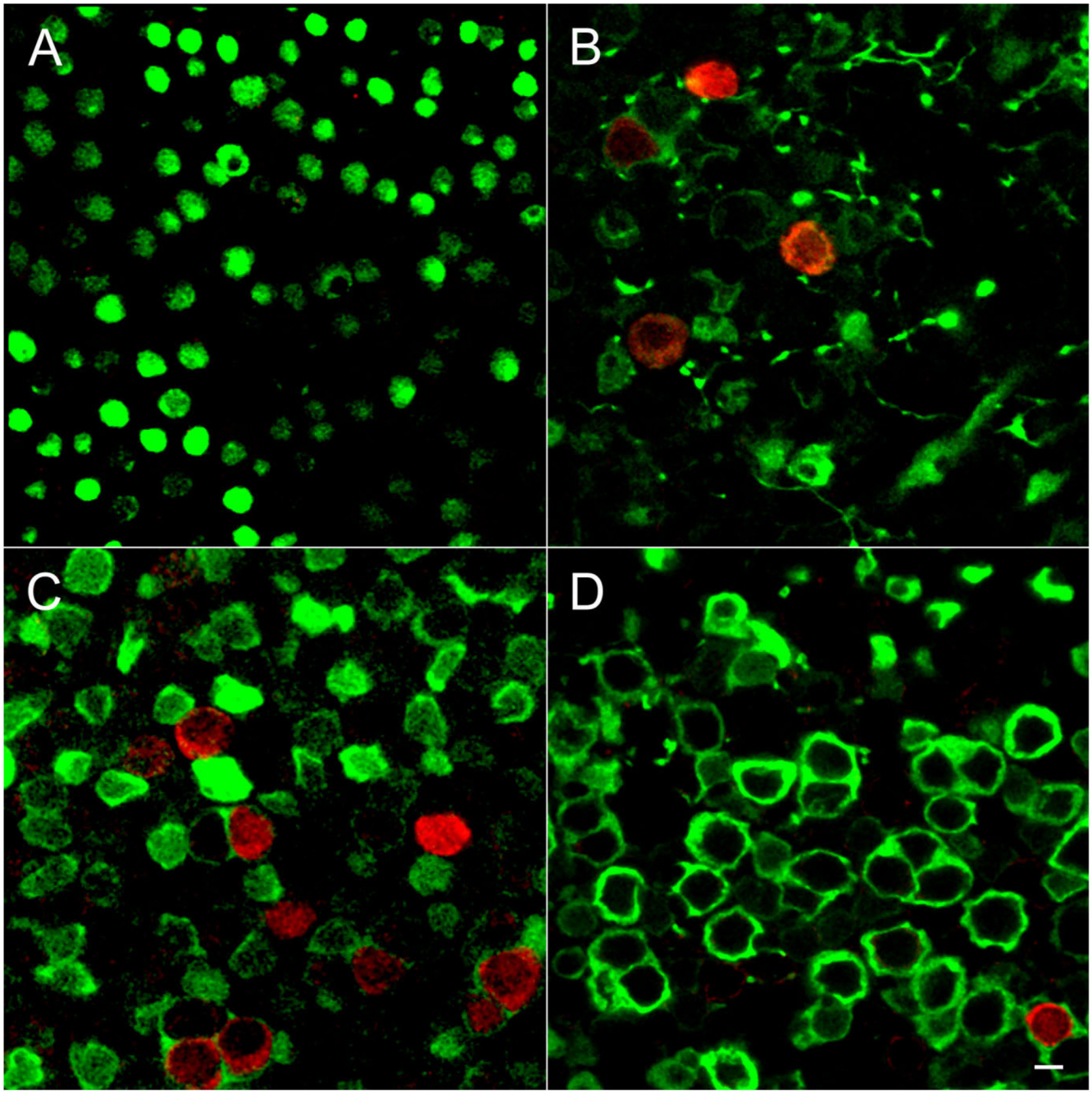

Figure 7.

Age-dependent expression of BK channels in the utricle. Whole-mount preparations of utricles were immunolabeled for BK (red) and calretinin (green). Single confocal sections taken from the striolar region are shown. **A:** At P6 calretinin-positive calyces are not well developed, making it difficult to identify the striolar region. However, no BK-positive hair cells were observed in any part of the epithelium. **B:** By P14 BK-positive hair cells are surrounded by calretinin-positive calyces. We rarely observed four BK-positive hair cells in a single field of view. **C:** By P21 many BK-positive hair cells engulfed in calretinin-positive calyces are present. **D:** By 2 months of age (P62) only a few BK-positive hair cells are evident. Scale bar = 5 μm in A–D.

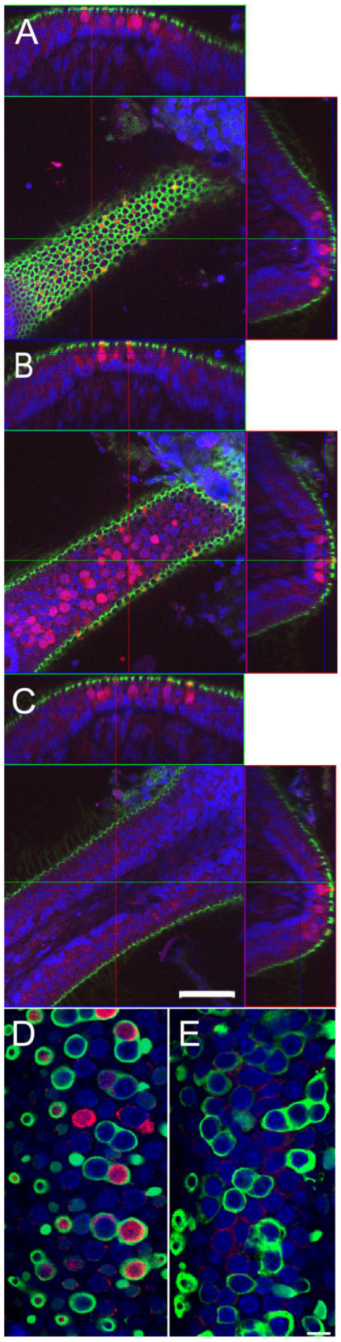

Figure 8.

BK channel expression in cristae ampullaris. A–C: A horizontal crista of a 3-week-old animal triple stained for actin (phalloidin; green), nuclei (NeuroTrace, blue) and BK (red) is shown. Optical confocal sections at different Z planes through a single crista are shown in the middle, and the reconstructed orthogonal sections along the XZ and YZ planes are shown on top and to the right of the XY plane, respectively. **A:** Confocal section through the top of the crista. Note the reticular appearance of the actin associated with tight junctions. BK-positive hair cells appear yellow in the center image due to the overlay of the green actin and red BK signal. **B:** Confocal section through the middle of hair cells at the apical portion of the crista. Note the numerous BK-positive hair cell bodies. **C:** No BK-positive

hair cells are found at the lateral edges of the crista. Note the actin-positive hair bundles perpendicular to the edge of the crista. In A–C, the cross-sectional reconstructions above and to the right of the images further illustrate the exclusive localization of BK-positive hair cells to the apical portion of the crista. **D:** Confocal section through the apical portion of a horizontal crista of a 3-week-old animal triple stained for BK (red), calretinin (green), and NeuroTrace (blue). Note the calretinin-positive calyces associated with many of the BK-positive hair cells. **E:** Confocal section through the apical portion of a horizontal crista of an adult animal. Note the absence of BK-positive hair cells. Scale bar = 50 μm in A–C; 10 μm in D,E.